OBSERVER DESIGN FOR UNDERWATER VEHICLES WITH POSITION AND ANGLE MEASUREMENT

Jon E. Refsnes [*1] **Kristin Y. Pettersen** [**]
Asgeir J. Sørensen [*]

[*] *Department of Marine Technology*
Norwegian University of Science and Technology (NTNU)
NO-7491 Trondheim, Norway
[**] *Department of Engineering Cybernetics, NTNU*

Abstract: In this paper we propose a new observer system for underwater vehicles. The main design objective behind this strategy is to reduce the destabilizing effect of the Coriolis and centripetal forces and moments in the observer. Especially for low cost vehicles with limited measurement equipment, these forces and moments represent a significant challenge for automatic control when the forward speed is sufficiently high. However, by explicitly utilizing an estimation of the current velocity in the observer, this paper shows that a high degree of robustness related to environmental disturbance and measurement noise is achieved. This is related to the estimation of the destabilizing Coriolis and centripetal forces and moments. UGES is proven for the observer error dynamics. Furthermore, this observer scheme has shown to be tolerant to large error in the position measurements, which is a common occurrence in underwater navigation.

Keywords: Low cost AUV, nonlinear observer, Munk moment, current estimation.

1. INTRODUCTION

For underwater vehicles moving with some forward speed, the dynamics, which often are described as Euler-Lagrange systems, are highly nonlinear and coupled. This presents control challenges that have led to a considerable interest on the tracking control performance of vehicles such as AUVs and ROVs over the last decades. Depending on the vehicle properties and control objective, there have been proposed a large variety of nonlinear control schemes that are derived using methods such as sliding mode, backstepping or feedback linearization. A common obstacle in many controller/observer designs has been how to dominate the destabilizing effects of the Coriolis forces and moments. Naturally, this problem alleviates as the number of sensors on board the vehicle and therefore feedback options in the control design increases. However, enhancing the sensor equipment causes increased costs and design complexity. Moreover, the capability of satisfactory performance despite sensor malfunctions is an attractive property in terms of reliability and in a fault-tolerant perspective.

The problem addressed in this paper is motivated by the Minesniper developed by Kongsberg ASA. The AUV/ROV, presented in Refsnes *et al.* (2005), is a low cost, torpedo shaped underwater vehicle. The low weight compared to the relatively high nominal speed implies that the dynamics are speed dominant and that the nonlinear characteristics of the hydrodynamics become decisive. Moreover, since it is designed with focus on low cost, it does not carry velocity sensors of any kind. Hence, an observer is needed to provide velocity estimates.

[1] This work is sponsored by NTNU and Kongsberg ASA, Norway.

Over the last decade, observers and output feedback control of underwater vehicles have been studied by numerous authors. A common method in observer design is to simplify the system model to some extent using valid assumptions that are made based on the vehicle properties and the mission task. In Aguiar and Pascoal (2002), a three DOF output feedback control system has been designed for the *Sirene* AUV using a kinematic observer for the current velocity. A three DOF observer of the vehicle dynamics is designed in Do *et al.* (2002), for the underwater vehicle ODIN, in which environmental disturbance is not considered. With focus on robustness to measurement noise, a six DOF global asymptotically stable observer is designed for underwater vehicles in Fossen and Fjellstad (1995). Inspired by this work, we have in this paper focused on developing a control plant model (CPM) with a corresponding observer based on hydrodynamic properties and robustness issues related to environmental disturbance, model uncertainty and measurement noise.

The main contribution of this paper is a pair of co-working nonlinear Luenberger observers. The observers provide global exponential stability of the error dynamics. Furthermore, this paper elaborates on the modelling of the destabilizing Coriolis and centripetal forces and moments. Simulations show that including the current velocity in the control plant model can lead to improved performance of the observer.

2. THE 6 DOF UNDERWATER VEHICLE PROCESS PLANT MODEL

The process plant model of an underwater vehicle can be described by the nonlinear model (Fossen, 2002)

$$\dot{\eta} = J(\Theta)\nu \tag{1a}$$

$$M\dot{\nu} + C_{RB}(\nu)\nu + C_A(\nu_r)\nu_r + D(\nu_r)\nu_r + g(\Theta) = \tau \tag{1b}$$

where $\eta = [x, y, z, \phi, \theta, \psi]^T$ denotes the Earth-frame position and orientation described by Euler angles. $M, C_{RB}, C_A, D \in \mathbb{R}^{6\times 6}$ represent the mass (included added mass), rigid-body Coriolis, added mass Coriolis and the damping matrix, respectively. The transformation matrix $J(\Theta)$ and the gravity vector $g(\Theta)$ are functions of the Euler angles $\Theta = [\phi, \theta, \psi]^T$. The velocity vector is given by $\nu = [u, v, w, p, q, r]^T$, which is defined in the body-frame. Assuming the current to be irrotational, it can be described by the vector $\nu_c^e = [\nu_x, \nu_y, \nu_z, 0_{1\times 3}]^T$ where ν_x, ν_y and ν_z denote the current components in North, East and down direction, respectively. The Earth-frame current vector is rotated into body-frame by $\nu_c = J^{-1}(\Theta)\nu_c^e$ where $\nu_c = [u_c, v_c, w_c, 0_{1\times 3}]^T$. Here, u_c, v_c and w_c represent the current velocity in surge, sway and heave respectively. The relative velocity vector is then given by $\nu_r = \nu - \nu_c$ in the body-frame.

2.1 Modelling of the Destabilizing Munk Moment

The Munk moment: "Any shape other than a sphere generates a moment when inclined in an inviscid flow. The Munk moment arises because of the asymmetric location of the stagnation points, where the pressure is highest on the front of the body (decelerating flow) and lowest on the back (accelerating flow). Due to this fact, the Munk moment is always destabilizing in the sense that it acts to turn the vehicle perpendicular to the flow." (Traiantafyllou and Hover, 2002)

A critical difference - $C_A(\nu)\nu$ vs. $C_A(\nu_r)\nu_r$: The effect of using the relative versus the vessel velocity in the added mass Coriolis matrix can most easily be seen by studying the Munk moment. Excluding the relative velocity in the model gives the following expression of the Munk moment in yaw

$$N_{Munk}(\nu) = (Y_{\dot{v}} - X_{\dot{u}})uv \tag{2}$$

whereas

$$N_{Munk}(\nu_r) = (Y_{\dot{v}} - X_{\dot{u}})u_r v_r \tag{3}$$

for models including the relative velocity. When there are ocean currents present, the vehicle will presumably drift with some speed in the same direction as the current unless this is compensated for by the controls. This applies to a large group of underwater vehicles with no controls in sway and heave. To underline this we use Fig. 1 where the sway velocity v and the relative sway velocity v_r, are depicted in a simulation with the Minesniper MkII. In this run, the vehicle moves along several straight paths with different orientation. The current is set to 0.5 m/s, and the forward speed $u = 2$m/s. Calculating the Munk moment using the velocities shown in the figure and given in the properties of Minesniper where $X_{\dot{u}} = -1.42$, $Y_{\dot{v}} = -38.4$, reveals a critical difference between (2) and (3). For the first 20 seconds of the run presented in Fig. 1, the sway velocity is approximately 0.25 m/s. Hence, the Munk moment generated by (2) is $N_{Munk}(\nu) \simeq 18.5$ Nm, whereas for (3) results in $N_{Munk}(\nu_r) \simeq 0$ Nm. Clearly, the Munk moment is overdimensioned when using (2). This error may increase the risk of poor tracking performance for tracking control schemes based on this model. Note that there are Munk moments in all the angular directions. We have in this section used yaw as an illustrative example.

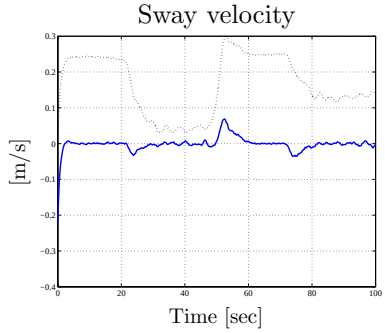

Fig. 1. Sway velocity v (dotted black) and relative sway velocity v_r (solid blue) versus time.

3. TWO SEPARATE CONTROL PLANT MODELS

Based on the observations made in the prior section, we propose the following observer scheme. We divide the CPM into two separate models.

CPM 1: This is an exact copy of the process plant model (1) except that a bias b is included.

$$\dot{\eta} = J(\Theta)\nu \tag{4a}$$

$$M\dot{\nu} + C_{RB}(\nu)\nu + C_A(\nu_r)\nu_r + D(\nu_r)\nu_r + g(\Theta) = \tau + J^{-1}(\Theta)b \tag{4b}$$

$$\dot{b} = -T^{-1}b + B_b n \tag{4c}$$

The bias b is modelled as a Markov process where T is a diagonal matrix of positive time-constants. The bias model is driven by some bounded noise n with a scaling matrix B_b. It is included to compensate for unmodelled dynamics and environmental disturbances. The current velocity vector ν_c is generated by CPM 2.

CPM 2: This is a vessel model that accounts for the main effects of the current loads. The key task of this model is to generate the current velocity vector ν_c, which is used in CPM 1.

$$\dot{\eta}_2 = J_1(\Theta)\nu_2 \tag{5a}$$

$$M_2\dot{\nu}_2 + D_2(\nu_2)\nu_2 = \tau_2 + J_1^T(\Theta)b_2 \tag{5b}$$

$$\dot{b}_2 = -T_2^{-1}b_2 + B_2 n \tag{5c}$$

where $\nu_2 = [u_2, v_2, w_2]^T$ represent the velocities in surge, sway and heave respectively and $\eta_2 = [x_2, y_2, z_2]^T$ denotes the position in the NED-frame. $M_2, D_2, T_2 \in \mathbb{R}^{3\times 3}$ are the top left matrices of M, D and T in (1b). In this CPM, the angular velocities are disregarded. This is clearly a simplification of the complete model described in (1). However, it means that we assume that the current forces that are due to the orientation of the vehicle are dominant to the current forces that originate from the vehicle's angular velocity. Thus, this model captures the main influence of the current. The bias b_2 denotes the slowly varying environmental disturbance. Furthermore, the relation between the current velocity and the velocity vector ν_2 is given by

$$u_c = u_2 - u_d,\ v_c = v_2,\ w_c = w_2 \tag{6}$$

where u_d denotes the desired forward speed. The equations for sway and heave in (6) are valid for fully actuated and underactuated vehicles because of thrust loss effects in sway and heave in transit (Faltinsen, 1990).

We have thus a pair of CPMs that functions as a basis for observer design. Some important advantages follow by this separation of the complete model and by explicitly utilizing the current velocity in the CPMs:

The hydrodynamic properties of the vehicle are taken into account when modelling the effects of the slowly varying environmental disturbance. In particular, the current velocity is included when deriving the damping and Coriolis forces and moments.

Position measurements can be contaminated by severe noise in underwater navigation. This may lead to large deviations in the velocity estimates due to large amplitudes in the output injection terms in the observer. When utilizing an estimator that does not include the current velocity, we see from (2) that the surge and sway velocities have direct influence on the calculation of the destabilizing Munk moment $N_{Munk}(\nu)$. Hence, large errors in sway direction may lead to large estimation errors in yaw velocity due to the strong coupling generated by the Munk moment. With the observer presented in Section 4, which is based on the pair of CPMs (4) and (5) using $N_{Munk}(\nu_r)$, the consequences of poor position measurements alleviates. This is because poor position measurements mainly lead to variations in the estimated body-fixed velocity $\hat{\nu}$ whereas the estimated relative velocity $\hat{\nu}_r$ will remain relatively unaffected and small. Hence, with this method, the calculation of the destabilizing Munk moment (3) is less dependent on the quality of the position measurements. This is an advantage in underwater vehicle applications.

4. OBSERVER DESIGN

In the following section we design a nonlinear Luenberger observer to each of the CPMs presented in the previous section. The observer design is based on the following assumptions:

A. 1. The position and angle vector η is measured.

A. 2. The velocity vector ν is bounded by V, i.e.

$$V = \sup_t \|\nu(t)\|\,,\ \ |\nu_i(t)| \le V_i \ \ \forall\ i \in \{1, .., 6\}$$

This is a common assumption in observer design, see e.g. Pettersen and Nijmeijer (1999).

We use the following notation in this paper. For any matrix $A(x) = A^T(x) > 0$ for all x, A_m and A_M denote the minimum and maximum eigenvalue of $A(x)$, respectively. Furthermore, the Euler angle symbol Θ is omitted in the following for notational simplicity.

Defining the following function $d(a) \triangleq D(a)a$, we have by using the mean value theorem $D(b)b - D(a)a = \frac{\partial}{\partial e} d(e)\Big|_{e=e_0}(b-a)$ where e_0 is on the line segment joining b and a. Moreover, we apply the following assumption:

A. 3. There exists a constant $\delta_m \in \mathbb{R}_+$ such that

$$\|\delta(e)\| \triangleq \left\| \frac{\partial}{\partial z} d(e)\Big|_{e=e_0} \right\| > \delta_m > 0$$

This implies that the hydrodynamic damping includes a linear term, e.g. $D(\nu)\nu = D_l\nu + D_{nl}(\nu)\nu$ where $D_l > 0$ is the linear damping matrix.
The following property yields:

P. 1. The transformation matrix can be expressed as $J = \text{diag}\{J_1, J_2\}$, where $\|J_1\| = 1$, and $J_M \triangleq \left\|J_2^{-1}\right\| = 2.173$.

To CPM 2, we define the following observer

$$\dot{\hat{\eta}}_2 = J_1\hat{\nu}_2 + L_2\tilde{\eta}_2 \tag{7a}$$

$$M_2\dot{\hat{\nu}}_2 + D_2(\hat{\nu}_2)\hat{\nu}_2 = \tau_2 + J_1^T(\hat{b}_2 + K_2\tilde{\eta}_2) \tag{7b}$$

$$\dot{\hat{b}}_2 = -T_2^{-1}\hat{b}_2 + K_{b2}\tilde{\eta}_2 \tag{7c}$$

where $L_2, K_2, K_{b2} \in \mathbb{R}^{3\times3}$ are positive definite and diagonal matrices. The estimated current velocity vector is obtained according to (6), i.e.

$$\hat{u}_c = \hat{u}_2 - u_d, \hat{v}_c = \hat{v}_2,\ \hat{w}_c = \hat{w}_2$$

Let the error vectors be defined as $\tilde{\eta}_2 \triangleq \eta_2 - \hat{\eta}_2, \tilde{\nu}_2 \triangleq \nu_2 - \hat{\nu}_2$ and $\tilde{b}_2 \triangleq b_2 - \hat{b}_2$. Subtracting (7) from (5) gives the following error dynamics

$$\dot{\tilde{\eta}}_2 = J_1\tilde{\nu}_2 - L_2\tilde{\eta}_2 \tag{8a}$$

$$M_2\dot{\tilde{\nu}}_2 = -\delta_2(e_2)\tilde{\nu}_2 + J_1^T(\tilde{b}_2 - K_2\tilde{\eta}_2) \tag{8b}$$

$$\dot{\tilde{b}}_2 = -T_2^{-1}\tilde{b}_2 - K_{b2}\tilde{\eta}_2 \tag{8c}$$

where we have assumed that the noise n is zero since the bias estimator is driven by estimation errors (Pettersen and Nijmeijer, 1999). The constant δ_2 refers to δ described in A.3. Following the same lines as for the analysis of the passive observer for dynamic positioning of ships presented in Fossen and Strand (1999), the origin $x_2 \triangleq [\eta_2^T, \nu_2^T, b_2^T]^T = 0$ of the error dynamics (8), is proven UGES by Lyapunov theory.

4.1 Vehicle Observer

In this section we derive a six-DOF nonlinear Luenberger observer for the vehicle dynamics. The CPM (4) is rewritten in Earth-frame coordinates as follows

$$\dot{\eta} = \nu^e = J\nu \tag{9a}$$

$$M^*\dot{\nu}^e + C^*_{RB}(\nu)\nu^e + C^*_A(\nu_r)\nu^e_r + D^*(\nu_r)\nu^e_r + g^* = J^{-T}\tau + b \tag{9b}$$

$$\dot{b} = -T^{-1}b + B_b n \tag{9c}$$

where $\nu^e = [\dot{x}, \dot{y}, \dot{z}, \dot{\phi}, \dot{\theta}, \dot{\psi}]^T$. For more details on the coordinate transformation, see Fossen (2002, Ch. 3.3).

Remark 1. When expressing the dynamics in the inertial frame (9), the matrices M^*, C^*_{RB}, C^*_A and D^*, and the vector g^* become functions of the transformation matrices J^{-1}, J^{-T} and $\frac{d}{dt}(J^{-1})$, which are all well defined for $\Theta \in \mathbb{R}^3$. That is, the use of J, which is undefined for $|\theta| = \frac{\pi}{2}$ is omitted from the system model. Hence, when implementing the observer using inertial coordinates, global stability results in $\mathcal{SO}(3)$ are obtainable. Note that $\hat{\nu}$ can be obtained by $\hat{\nu} = J^{-1}\dot{\hat{\eta}}$. However, when deriving a model based controller, body-fixed coordinates are needed which implies singularity for $|\theta| = \frac{\pi}{2}$ when using Euler angles.

P. 2. The mass matrix M^* is positive definite.

P. 3. The linear dependence on ν in $C(\nu) = C_{RB}(\nu) + C_A(\nu)$ gives that $\forall x, y \in \mathbb{R}^6$ and $\forall\alpha \in \mathbb{R}$, we have that

$$C(x + \alpha y)z = C(x)z + \alpha C(y)z$$

Furthermore, there exists a constant $C^*_M > 0$ such that

$$\|C^*(x)\| \leq C^*_M \|x\|$$

Inspired by Celani (2005) we propose the following observer

$$\dot{\hat{\eta}} = \hat{\nu}^e + \lambda L\tilde{\eta} \tag{10a}$$

$$M^*\dot{\hat{\nu}}^e + E^*(\sigma_V(\hat{\nu}))\sigma_V(\hat{\nu}^e) + g^* = J^{-T}\tau + \hat{b} + \lambda^2 M^* K\tilde{\eta} + A^*(\hat{\nu}_c)\hat{\nu}^e_r + A^*(\hat{\nu})\hat{\nu}^e_c \tag{10b}$$

$$\dot{\hat{b}} = -T^{-1}\hat{b} + \kappa\lambda^2 K_b\tilde{\eta} \tag{10c}$$

where $\lambda, \kappa > 0$ are constant scalars and $L, K, K_b \in \mathbb{R}^{6\times6}$ are positive definite and diagonal matrices. The error vectors yield $\tilde{\eta} \triangleq \eta - \hat{\eta}, \tilde{\nu}^e \triangleq \nu^e - \hat{\nu}^e$ and $\tilde{b} \triangleq b - \hat{b}$. Moreover, to simplify the notation, we have defined the following matrix $\forall m, n \in \mathbb{R}^6$

$$E^*(m)n \triangleq C^*(m)n + D^*(m)n$$

$$A^*(m)n \triangleq C^*_A(m)n + D^*(m)n$$

The function $\sigma_V(\cdot)$ is a component-wise saturation function with vector saturation level V; specifically, given $Y \in \mathbb{R}^6$ such that $Y_i \geq 0\ i = 1, .., 6$, $\sigma : \mathbb{R}^n \to \mathbb{R}^n$ is defined as follows

$$\sigma_Y(x_i) = \begin{cases} x_i & \text{if } |x_i| \leq Y_i \\ Y_i & \text{if } x_i > Y_i \\ -Y_i & \text{if } x_i < -Y_i \end{cases} \tag{11}$$

Subtracting (10) from (9) gives the following error dynamics

$$\dot{\tilde{\eta}} = \tilde{\nu}^e - \lambda L\tilde{\eta} \tag{12a}$$

$$M^*\dot{\tilde{\nu}}^e + E^*(\sigma_V(\nu))\nu^e - E^*(\sigma_V(\hat{\nu}))\hat{\nu}_e = \tilde{b} - \lambda^2 M^* K\tilde{\eta} - (A^*(\nu_c) + \bar{A}^*(\nu_c))\tilde{\nu}^e + G^*_p\tilde{\nu}^e_c \tag{12b}$$

$$\dot{\tilde{b}} = -T^{-1}\tilde{b} - \kappa\lambda^2 K_b\tilde{\eta} \tag{12c}$$

where we have defined the matrix $\bar{A}^*(n)m = A^*(m)n$. Moreover, the perturbation matrix G^*_p yields

$$G^*_p = -A^*(\nu) - \bar{A}^*(\nu) + A^*(\tilde{\nu}) + \bar{A}^*(\tilde{\nu}) + A^*(\nu_c) + \bar{A}^*(\nu_c) - A^*(\tilde{\nu}_c) \tag{13}$$

Similarly to Celani (2005), we define the following error vectors $\varepsilon_1(t) \triangleq \frac{1}{\lambda}\tilde{\eta}$, $\varepsilon_2(t) \triangleq \frac{1}{\lambda^2}\tilde{\nu}^e$, $\varepsilon_3(t) \triangleq \frac{1}{\kappa\lambda^2}\tilde{b}$. The nominal error dynamics, which is the complete error dynamics (12) excluding the perturbation term $G^*_p\tilde{\nu}^e_c$, can then be written in

the following compact form

$$\dot{x}_1 = \lambda G x_1 + \begin{bmatrix} 0_{6\times1}^T & f^T(\cdot) & 0_{6\times1}^T \end{bmatrix}^T \tag{14}$$

where

$$G = \begin{bmatrix} -L & I_{6\times6} & 0_{6\times6} \\ -K & 0_{6\times6} & 0_{6\times6} \\ -K_b/\kappa & 0_{6\times6} & -T^{-1}/\lambda \end{bmatrix}, \; x_1 \triangleq \begin{bmatrix} \varepsilon_1 \\ \varepsilon_2 \\ \varepsilon_3 \end{bmatrix}$$

and

$$f(\cdot) = \frac{M^{*-1}}{\lambda^2}[E^*(\sigma_V(\nu))\nu_e - E^*(\sigma_V(\hat{\nu}))\hat{\nu}_e - (A^*(\nu_c) + \bar{A}^*(\nu_c))\tilde{\nu}^e + \tilde{b}]$$

Since G is Hurwitz regardless of λ and κ we let S be the solution of the Lyapunov equation $G^TS + SG = -Q$ and propose the following Lyapunov function candidate $V_1 = x_1^TSx_1$. Differentiating V_1 along the state solutions yields

$$\dot{V}_1 = -\lambda x_1^TQx_1 + 2x_1^TS[\,0_{6\times1}^T \;\; f^T(\cdot) \;\; 0_{6\times1}^T]^T \tag{15}$$

Then, by Shim *et al.* (2001, Lemma 2) and P.3 we have that

$$\left\|E^*(\sigma_V(\nu))\nu_e - E^*(\sigma_V(\nu_e + \lambda^2\varepsilon_2))\right\| \leq \lambda^2 B \left\|\varepsilon_2\right\|$$

where $B > 0$ under A.2. Hence, we get that

$$\|f(\cdot)\| \leq \frac{1}{M_m^*}\{(\tilde{A}_{V_c}^* + B)\left\|\varepsilon_2\right\| + \kappa\left\|\varepsilon_3\right\|\} \leq W\left\|x_1\right\| \tag{16}$$

where $\tilde{A}_{V_c}^* \triangleq (A_M^* + \bar{A}_M^*)V_c$, $W \triangleq \frac{1}{M_m^*}(\tilde{A}_{V_c}^* + B + \kappa)$ and $V_c = \sup_t \|\nu_c(t)\|$. Consequently, we arrive at the following upper bound

$$\dot{V}_1 \leq -\left\|x_1\right\|^2(\lambda Q_m - 2S_MW) \tag{17}$$

By Lyapunov theory it follows that if

$$\lambda > 2S_MW/Q_m \tag{18}$$

the origin of the nominal observer error dynamics (14) is globally exponentially stable (GES).

We now proceed by showing stability of the overall system, which can be written in the following compact form

$$\dot{x}_1 = f_1(t, x_1) + g(t, x_1, x_2)x_2 \tag{19a}$$
$$\dot{x}_2 = f_2(t, x_2) \tag{19b}$$

where $\dot{x}_1 = f_1(t, x_1)$ represents the nominal system (14), and $\dot{x}_2 = f_2(t, x_2)$ denotes the current estimation error dynamics (8). The perturbation matrix yields

$$g(t, x_1, x_2) = \begin{bmatrix} 0_{6\times3} & G_p^*hJ_1 & 0_{6\times3} \\ 0_{6\times3} & 0_{6\times3} & 0_{6\times3} \end{bmatrix}^T \tag{20}$$

where $h = [I_{3\times3}, 0_{3\times3}]^T$. Let the complete error state be defined as $x \triangleq [x_1^T, x_2^T]^T$. We proceed with the main result of this paper.

Theorem 1. The origin $x = 0$ of the cascaded system (19) is UGES under A.1-3 and if (18) is satisfied.

Proof: The proof is based on Panteley *et al.* (1998). The origin of the systems $\dot{x}_1 = f_1(t, x_1)$ and $\dot{x}_2 = f_2(t, x_2)$ are shown GES and UGES, respectively provided that (18) is satisfied. The perturbation matrix can, by employing P.1 and P.3, be upper bounded according to

$$g(t, x_1, x_2) \leq (A_M^* + \bar{A}_M^*)(V + J_M\left\|\tilde{\nu}^e\right\|) + (A_M^* + \bar{A}_M^*)V_c + A_M^*\left\|\tilde{\nu}_c\right\|$$

under A.2. Furthermore, using that $\|\tilde{\nu}_2\| \leq \|x_2\|$ and $\|\tilde{\nu}^e\| \leq \|x_1\|$ and defining the following constants

$$\theta_1 \triangleq J_M(A_M^* + \bar{A}_M^*), \quad \theta_2 \triangleq A_M^*\left\|x_2\right\|$$

where $\theta_1, \theta_2 : \mathbb{R}_{\geq0} \to \mathbb{R}_{\geq0}$, we have that the perturbation vector can be upper bounded by

$$\|g(t, x_1, x_2)x_2\| \leq \theta_1(\|x_2\|)\left\|x_1\right\| + \theta_2(\|x_2\|)$$

Hence, the linear growth restriction on x_1 in the perturbation term is satisfied. Finally, since $x_2 = 0$ is UGES, we have that the origin of the cascaded system (19) is UGES.

□

5. CASE STUDY: THE MINESNIPER MKII

The simulations are carried out on the Minesniper MkII with 0.5 m/s current with direction 90°. The forward speed is set to 1.5m/s. White noise is added to the state measurements η, which are updated at Minesniper MkII frequencies. To test the robustness further, the observer damping coefficients are only 80% of the actual coefficients in the process plant model. Figure 2 shows the estimation error.

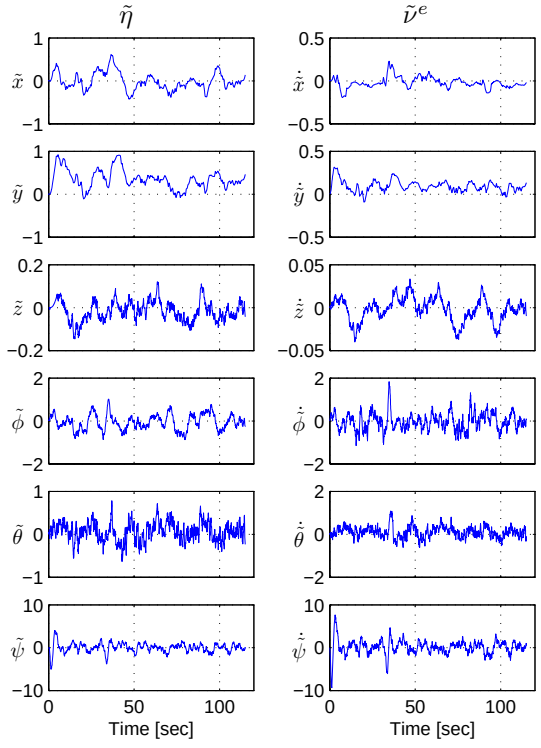

Fig. 2. Left: Estimation error $\tilde{\eta}(t)$ in [m],[deg]. Right: Estimation error $\tilde{\nu}^e(t)$ in [m/s],[deg/s].

The top left plot in Fig. 3 presents the horizontal position for the simulated run. Furthermore, the right plots present the estimated current velocity and direction, which reveals a relatively large deviation in the current estimation. In spite of this, it is shown in the bottom plot that improved results are obtained using this observer scheme compared to an observer without explicit current estimation. The bottom plot depicts the $\mathcal{L}_2$-norm of the estimation error obtained in two simulations runs with identical control inputs, environmental conditions and observer gains/coefficients. The

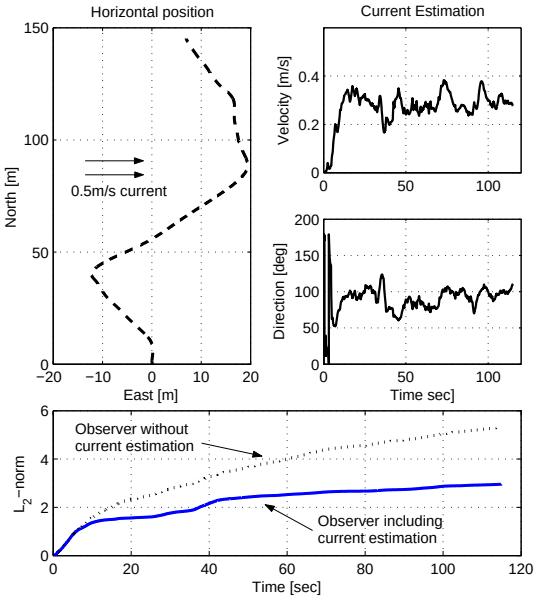

Fig. 3. Top left: Horizontal position. Top right: Estimated Current velocity. Middle right: Estimated current direction. Bottom: Comparison of the $\mathcal{L}_2$-norm.

bottom plot in Fig. 3 indicates that including the relative velocity in the observer decreases the estimation error. This is mainly due to the more accurate estimation of the destabilizing Munk moment. Although the amplitude of the norm presented in Fig. 3 is dependent on the choice of observer gains, we experienced similar results for a large number of simulations.

6. CONCLUSION

An observer system for underwater vehicles has been developed. It consists of a pair of nonlinear and co-working Luenberger observers. The observer provided accurate state estimation with the inclusion of the nonlinear Munk-moment accounting for the current velocity. Furthermore, comparing this with an equivalent observer excluding the current velocity indicated improved results. These advantages give reason to describe this as a robust model for control of underwater vehicles in the sense that it is insensitive to environmental disturbance and measurement noise.

7. ACKNOWLEDGEMENTS

The authors would like to thank Kongsberg ASA for their support and contribution to the project.

REFERENCES

Aguiar, A. P. and A. M. Pascoal (2002). Dynamic positioning and way-point tracking of underactuated AUVs in the presence of ocean currents. In: *Proc. 41st IEEE Conf. Decision & Control*. Las Vegas, Nevada, USA. pp. 2105–2110.

Celani, F. (2005). An asymptotic observer for robot manipulators with position measurements. arXiv math.OC/0507072.

Do, K. D., Z. P. Jiang, J. Pan and H. Nijmeijer (2002). Global output feedback universal controller for stabilization and tracking of underactuated ODIN-an underwater vehicle. In: *Proc. 41st IEEE Conf. Decision & Control*. Las Vegas, NV, USA. pp. 504–509.

Faltinsen, O. M. (1990). *Sea Loads on Ships and Ocean Structures*. Cambridge University Press.

Fossen, T. I. (2002). *Marine Control Systems: Guidance, Navigation and Control of Ships, Rigs and Underwater Vehicles*. Marine Cybernetics. Trondheim, Norway. http://www.marinecybernetics.com.

Fossen, T. I. and J. P. Strand (1999). Passive Nonlinear Observer Design for Ships Using Lyapunov Methods: Full Scale Experiments with a Supply Vessel. *Automatica* **35**(1), 3–16.

Fossen, T. I. and O. E. Fjellstad (1995). Robust adaptive control of underwater vehicles. In: *In Proc. 3rd IFAC Workshop on Control Applications in Marins Systems (CAMS95)*. Trondheim, Norway. pp. 66–74.

Panteley, E., E. Lefeber, A. Loría and H. Nijmeijer (1998). Exponential tracking control of a mobile car using a cascaded approach. In: *Proc. IFAC Workshop on Motion Control*. Grenoble, France. pp. 221–226.

Pettersen, K. Y. and H. Nijmeijer (1999). Output feedback tracking control for ships. In: *Lecture Notes in Control and Information Science 244, New Directions in Nonlinear Observer Design*. pp. 311–334. Springer. Nijmeijer, H. and Fossen, T. I. (Eds).

Refsnes, J. E., A. J. Sørensen and K. Y. Pettersen (2005). Design of output feedback control system for high speed maneuvering of an underwater vehicle. In: *Proc. MTS/IEEE, OCEANS*. Washington D.C., USA.

Shim, H., Y. I. Son and J. H. Seo (2001). Semi-global observer for multioutput nonlinear systems. *Systems and Control Letters* **42**(3), 233–244.

Traiantafyllou, M. S. and F. S. Hover (2002). Maneuvering and control of marine vehicles. Technical report. Department of Ocean Engineering, Massachusetts Institue of Technology. Cambridge, Massachusetts, USA.